Journal of Hydrology 625 (2023) 129974

Contents lists available at ScienceDirect

Journal of Hydrology

journal homepage: www.elsevier.com/locate/jhydrol

Research papers

Integration of physically-based numerical tools and socio-hydrological variables in urban flood modeling

Leyner Cardenas-Mercado [a,b,*], Jorge Escobar-Vargas [a], Jhonny I. Pérez-Montiel [b], Andres Torres [c]

[a] Department of Civil Engineering, School of Engineering, Pontificia Universidad Javeriana, Bogotá, Colombia
[b] Grupo de Investigación GISA, Facultad de Ingeniería, Universidad de La Guajira, Km 5 Vía a Maicao, Riohacha 440007, Colombia
[c] Instituto Javeriano del Agua, Pontificia Universidad Javeriana, Bogotá, Colombia

ARTICLE INFO

This manuscript was handled by Emmanouil Anagnostou, Editor-in-Chief

Keywords:
Physics-based modeling
Support vector machines
Flood model optimization
Model integration
Pluvial flood

ABSTRACT

Floods are considered the most destructive natural catastrophes on the planet; therefore, studying their dynamics in the context of each region is a fundamental pillar of society. A very popular tool for studying the degree of threat is physics-based modeling using 2D models. It is imperative to include physical, hydrological, and anthropogenic variables in flood modeling approaches. The reviewed literature did not develop a methodology or strategy to facilitate this process. Based on this reason, it was considered for Riohacha, a coastal city in northern Colombia. A survey was conducted to determine social, economic, and flood depth variables during extreme events. Twenty socio-hydrological variables were obtained from the survey analysis using Kruskal–Wallis and multiple correspondence analysis (MCA) tests. Flood depth was the response variable used to select the socio-hydrological variables, among which the following stood out: age of the house, internal slope, toilet overflow, proximity to a wetland, paved road, raft area, and slope of the soil in front of the house. An iterative process supported by a Support Vector Machine (SVM) dummy was used to determine the appropriate combination of parameters and optimize the calibration process of the TELEMAC-2D hydrodynamic model. The curve number (CN) and Manning friction coefficient were used as calibration parameters. The optimization process was performed by entering the dummy SVM into the socio-hydrological variables CN and Manning's n to test up to 20,000 possible combinations of the parameters and evaluate the mean absolute error (MAE), mean error (ME), absolute relative error (RAE), root mean square error (RMSE), and inertia root mean squared error (IRMSE). The best combination of parameters to simulate an extreme flood event and determine the metrics with the observed and simulated flood depths was entered into TELEMAC-2D. This paper presents a methodological proposal for optimizing the calibration process of physics-based flood models (traditional method), considering socio-hydrological variables, to articulate it as a new step in the modeling protocol. In the traditional simulation, an RMSE of 0.48 m, MAE of 0.37 m, and IRMSE of 1.37 m are obtained, which decrease to 0.33 m, 0.27 m, and 0.92 m, respectively, when the socio-hydrological variables are included. Contrary to the previous metrics, the ME improves slightly from 0.15 m with the traditional method to 0.17 m when the socio-hydrological variables are included. These results can be improved using a digital terrain model (DTM) that more realistically represents the complexity of the urban fabric. With only 7 iterative processes, the model calibration was optimized using only seven iterative processes. Therefore, the proposed methodology was established as a tool for optimizing the flood modeling processes.

1. Introduction

Floods are among the most common and highly impactful natural hazards worldwide, resulting in loss of life and economic damage in areas with high population densities, financial and industrial activities, historical centers, and road systems (Minano et al., 2021; Zambrano et al., 2018). Flooding events in urban centers have increased because of extreme rainfall caused by climate change, poor drainage systems, and

* Corresponding author.
E-mail addresses: cardenas-leyner@javeriana.edu.co (L. Cardenas-Mercado), jorge-escobar@javeriana.edu.co (J. Escobar-Vargas), jpemon@uniguajira.edu.co (J.I. Pérez-Montiel), andres.torres@javeriana.edu.co (A. Torres).

https://doi.org/10.1016/j.jhydrol.2023.129974
Received 13 December 2022; Received in revised form 12 July 2023; Accepted 16 July 2023
Available online 20 July 2023
0022-1694/© 2023 The Author(s). Published by Elsevier B.V. This is an open access article under the CC BY license (http://creativecommons.org/licenses/by/4.0/).

impervious areas, which are becoming increasingly prevalent in urban areas (Nkwunonwo et al., 2019).

Anthropogenic factors, such as solid waste, can aggravate flooding by blocking storm drains, which is common in cities and towns in developing countries (Anh & Ngoc, 2019; Nwe Aung et al., 2019). As with all structural measures, the designed capacities of drainage systems limit their efficiency when the capacity of the system is exceeded, and flooding occurs along with heavy rainfall runoff, thereby causing significant damage (Agonafir et al., 2022; Habibi & Seo, 2018; Yan et al., 2018).

The components used to identify flood hazards include water depth, duration, velocity, sediment content, and probability of occurrence (Abebe et al., 2019). Mathematical models based on physics are the most commonly used approaches to assess these hazards (Mignot et al., 2019). Owing to computational developments, various models have been implemented to represent the behavior of urban flooding in 1D, 2D, or coupled 1D/2D (Nardini & Miguez, 2016; Pérez-Montiel et al., 2022; Russo et al., 2015; Shen et al., 2019). However, depth-averaged models (Kundu et al., 2015) have several limitations, as they can only include the processes that the governing equations allow them to represent, such as precipitation, runoff, velocity, free surface elevation of the fluid, soil erosion, and sediment transport (Wan Mohtar et al., 2020), and they require a high computational cost to solve the equations (De Goede, 2020; Juez et al., 2014; Kim et al., 2014; Lu & Wai, 1998; Luo et al., 2022). If we add to these limitations, the limited information on observed data on water depth during extreme events, flood extent, and coverage, among others, increases the complexity of the modeling exercise (Martins et al., 2018; Mignot et al., 2019).

According to Neal et al. (2012), factors less obvious than physical complexity can lead to significant differences between the simulation results and observations. In this sense, flood magnitude depends not only on total rainfall intensity and duration but also on land use, topography, urban development, wetland modifications, and anthropogenic environments (Abebe et al., 2019; Dahri & Abida, 2020). Among these factors, in urban flood modeling, the anthropogenic component has been studied from a socio-hydrological perspective, which seeks to analyze the understanding and dynamics at different spatial and temporal scales to discern the underlying characteristics of biophysical and human systems and their interactions (Blair & Buytaert, 2016). This makes it possible to understand the dynamics and co-evolution of the human-water system and study the impact of people on water, and vice versa (Genova & Wei, 2023; Khalifa et al., 2020; Massuel et al., 2018; Mostert, 2018).

Studies on urban floods using a socio-hydrological approach have considered anthropogenic variables such as relative flood damage, relative population density, collective memory, communicative memory, and cultural memory to understand this phenomenon from a holistic perspective (Buarque et al., 2021; Ciullo et al., 2017; Song et al., 2021). Buarque et al. (2021) presented an analytical framework for flood risk assessment using a socio-hydrological approach and integrated it with an urban flood model using a Cellular Automata approach and climate projections. Di Baldassarre et al. (2015) proposed a set of differential equations for the dynamic modeling of changes in flood risk to understand the joint dynamics of floods and societies, becoming a social response to floods. Despite these approaches, in most flood studies based on hydrodynamic models, the variables associated with anthropogenic behavior are not usually considered because of the limitations of the equations that support them (Abebe et al., 2019). The first approximation was made by Du et al. (2023); however, the socio-hydrological variables were not included in the hydrodynamic model, nor were they directly related to it. They were used through the combination of three models: (1) a hydrodynamic model for flood simulation, (2) an agent-based model for evacuation management policies and human behaviors, and (3) a transportation model to study the evacuation processes of houses in a road network before flood events in the city of Xiong, China.

One of the most popular machine learning algorithms used to study and predict flooding behavior is Support Vector Machine (SVM), which is a binary supervised learning classifier (J Liu et al., 2021). This tool has been used to evaluate the correlation between the occurrence of floods and the factors that condition these events (Tehrany et al., 2014); generate flood susceptibility maps (Jun Liu et al., 2022); produce spatial models for flood susceptibility assessment (Tehrany et al., 2015); and optimize particle swarm models for flood forecasting (Anupam & Pani, 2020). However, in the consulted literature, no parameter optimization, including social variables in flood modeling or the interaction between physics-based models and statistical models, was identified.

It is imperative to include all the physical, hydrological, and anthropogenic variables that influence this phenomenon in flood modeling approaches. However, the integration of these variables into a single modeling framework has not yet been proposed; therefore, despite its applicability to a wide range of real cases, a methodology to facilitate the process has not been developed. This article presents a methodological proposal for optimizing the calibration process of physics-based flood models, considering socio-hydrological variables as a new step in the modeling protocol. The case study is the city of Riohacha, a coastal city located in the north of Colombia where basic starting information is available. It was previously known for its great susceptibility to flooding in the face of extreme events, inadequate solid waste management, and poor population habits.

2. Materials and methods

2.1. Case study

This study involved the Riohacha district, Riohacha, the capital of the department of La Guajira, Colombia. The urban area has an approximate population of 287,000 and a surface area of 3,080 km^2 (CDGRD, 2019). The study area covers 19.48 km^2 (Fig. 1) and is called an urban sub-basin. Riohacha has several environmental characteristics, including the Ranchería River delta, a branch called Riito, a mangrove forest, and a series of wetlands. All of these particularities are related and interact in the urban sub-basin, which is the delimitation of the modeling area, as shown in Fig. 1. The “winter wave,” an extreme flood event that affected most of the Colombian territory in 2010–2011, associated with the La Niña phenomenon (Campuzano et al., 2015), severely impacted Riohacha, flooding several areas and causing significant damage to the infrastructure and to the inhabitants (Nardini & Miguez, 2016; Pérez-Montiel et al., 2022).

The occurrence of floods in Riohacha is attributed to climate. However, the problem rests with poor planning of the Old Town and uncontrolled urban development. Apart from the increase in impervious surfaces, the principal natural thalweg of the urban watershed has been interrupted by urbanization and the partial, progressive earth-filling of the wetlands themselves to conquer new spaces for building houses (Nardini & Miguez, 2016). The drainage system fails because of hydraulic constraints, and the retention volumes diminish. Coastal regions are particularly susceptible to flooding given their exposure to storm surges, tsunamis, and especially the terrain’s low slope (Ning et al., 2018), which, in turn, is another aggravating factor for floods in Riohacha.

Floods are also aggravated by i) the removal of sewer cover when precipitation occurs, ii) inadequate handling of garbage that blocks sewers, and iii) the presence of the sea, determining the lowest drainage level for the Ríito and Laguna Salada, which eventually affects the entire upstream system due to backwater effects (Nardini & Miguez, 2016). In addition, Riohacha was selected for this study, given the diversity of information available on flood events. The database used in this study was built using primary information from topographic surveys and secondary sources, principally the Centro De Recuperación De Ecosistemas Acuáticos (CREACUA), the company responsible for managing sewage systems, and the Instituto de Hidrología, Meteorología y

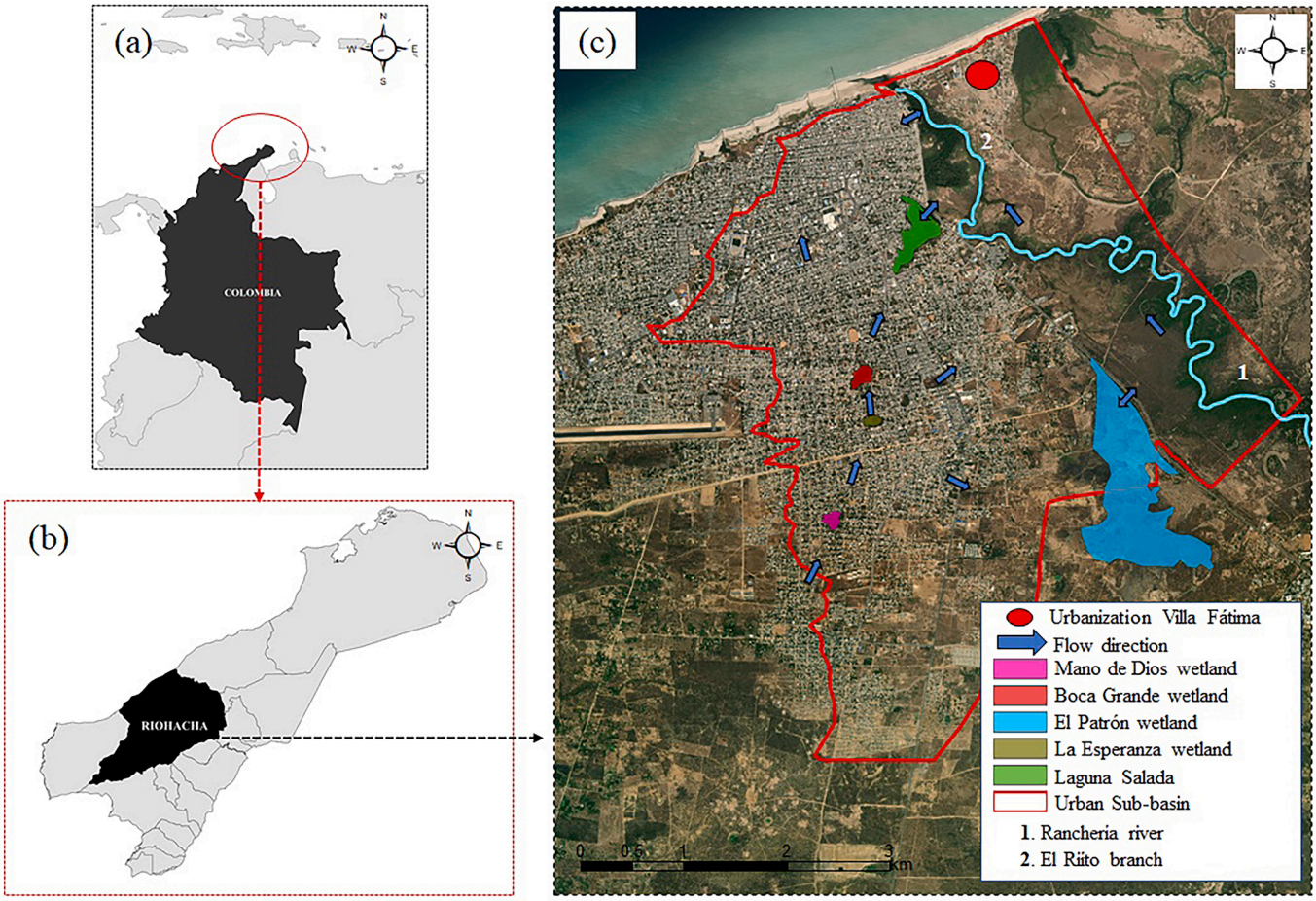


Fig. 1. Delimitation of the study area. (a). Location of the department of La Guajira in Colombia; (b). Location of Riohacha in La Guajira; (c). Delimitation of the urban sub-basin and generalities of the runoff.

Estudios Ambientales (IDEAM).

2.2. Meteorological variables

Flooding in the city of Riohacha, the subject of this study, is caused by pluvial flooding. In this case, the input variable was the precipitation represented in a hyetogram (mm/h) of the extreme events considered on September 18, 2011 (return period of 87 years and intensity of 231 mm/d) and November 29, 2011 (return period of 10 years and intensity of 150 mm/d). In both cases, the hyetograms had a duration of 3 h and were discretized every 5 min, thus capturing the behavior of each event. The precipitation data available are from the IDEAM rain gauge at the Almirante Padilla station in Riohacha. (Pérez-Montiel et al., 2022).

2.3. Hydraulic variables

The hydraulic variables considered were: (i) initial condition of the wetlands and water depth; (ii) base flow of the El Ríito arm on the day of the flood event; (iii) altimetric information incorporated with the digital terrain model (DTM) of 5 m horizontal resolution, corrected with control points and verification of altimetric data taken with fieldwork and the help of a GPS-RTK (Real Time Kinematic); (iv) shapefiles and ortho-photo of the study area; (v) dimensions and characteristics of the most relevant hydraulic structures to study flooding in the urban sub-basin.

3. Methodological development

Fig. 2 shows the proposed methodology for Step 1. Socio–hydrological variables: Step 2. Mathematical model based on physics: Step 3. Calibration strategy using the results of Steps 1 and 2.

3.1. STEP 1 - socio-hydrological variables

Social, economic, and flood height data were obtained from a survey previously developed to determine the impact of the floods of the 2010–2011 winter wave, the period during which the extreme events considered in this study occurred (CREACUA, 2013). A total of 411 surveys were administered to an equal number of households distributed proportionally according to the population in the area of interest (Pérez et al., 2018a). The socioeconomic information collected included the physical characteristics of the dwellings, income level, solid waste management, historical flooding, flood depth, duration of flooding, and the number of people affected by flooding (Nardini & Miguez, 2016; Pérez et al., 2018a). The socio-hydrological variables identified in this methodological proposal arise from the analysis of the survey and DTM analysis, not from the formulation or execution of the methodology of CREACUA (2013).

The survey results were analyzed to find correlations with the response variable (flooding depth), which are not necessarily cause–effect relationships. In this sense, the following techniques were applied: i) univariate analysis using the Kruskal-Wallis test, which is a non-parametric statistical method to study whether different data come from the same population, working only with categorical data (Monge, 2019); and ii) multiple correspondence analysis (MCA), a statistically based visualization method that allows the user to represent and analyze associations between categorical variables graphically (Esmaelian et al.,

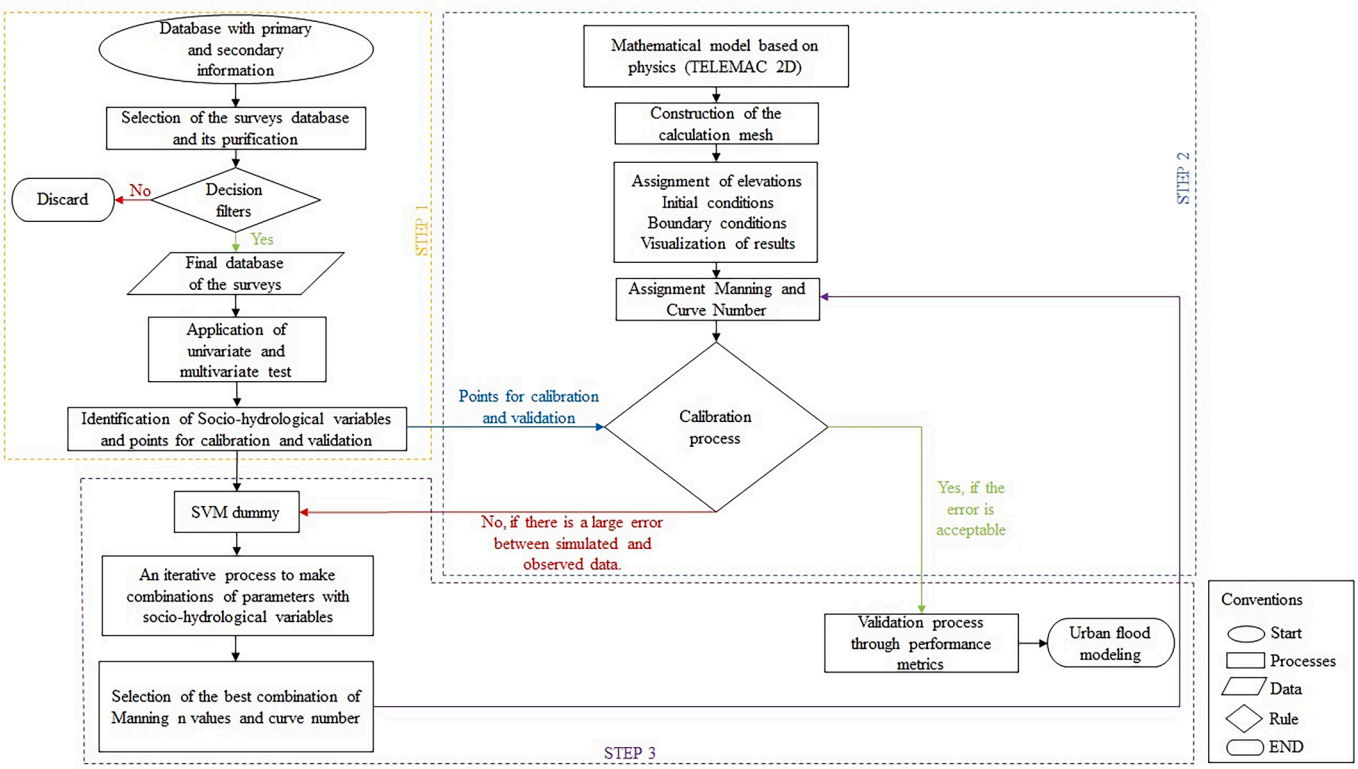


Fig. 2. Diagram of the methodological process followed in the development of the research.

2017; Shao-Zhong Zhang et al., 2002). The variables that could provide statistical information on the behavior of flood depth (greater or lesser depth) were categorized as socio-hydrological variables owing to the influence of socio-cultural aspects, which allowed us to understand the dynamics of the human-water system in the face of flood events. For the application of univariate and multivariate tests, the numerical variables

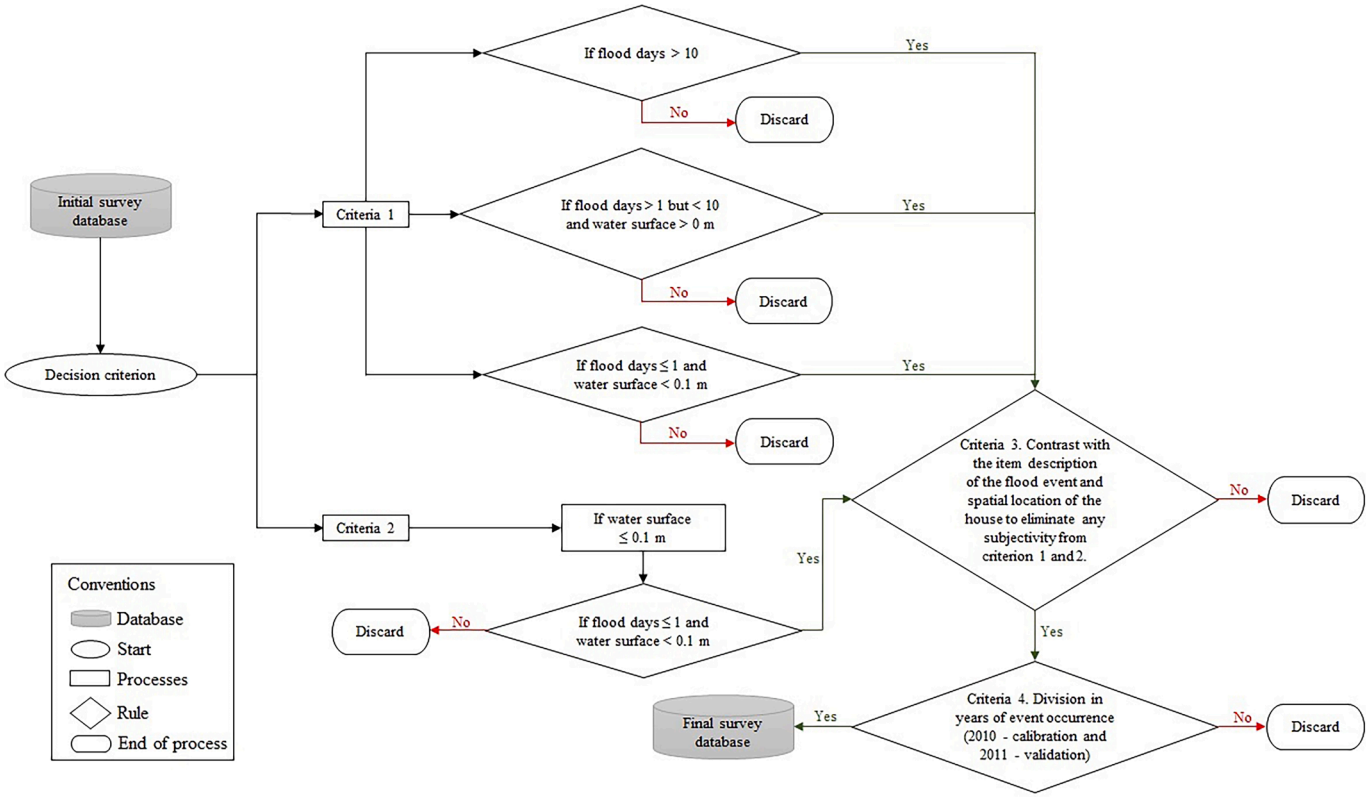


Fig. 3. Criteria for selecting the survey database to be studied.

in the database were categorized using box-plot analysis (Pathak, 2014). To categorize variables of two levels (e.g., solid waste collection, paved streets, toilet overflow), the first quartile and median were used; the median value and third quartile were considered for variables with three or more levels.

As the survey was conducted several years after the events, it was necessary to clean the survey before defining the socio-hydrological variables and selecting calibration points. The time between the event and the survey (four years) could have influenced the results because of forgetfulness and even the expectation of receiving compensation for damages suffered in historical flood events. Under this approach, observations that presented inconsistencies, mainly unrealistic flood depths and locations of houses in high-elevation areas, were excluded. The criteria and processes used to discard observations from the survey are presented in Fig. 3.

As shown in Fig. 3, Criterion 1 identifies the observations that are affected by the days of the event duration and flood depth. Criterion 2 assessed the consistency between the existence of an event, the duration of the event, and flood depth. Criterion 3 contrasts the flood depth with the description of the flood event (textual and narrated description of the event experienced by the interviewee) and the spatial location of the dwelling (proximity to the wetland and topographic location). The calibration (32 observations) and validation (31 observations) points were obtained using Criterion 4, which classified the observations accepted by each filter by the date of occurrence of the events (September and November 2011).

3.2. STEP 2 - physics-based mathematical model

The mathematical model implemented in this research was the shallow water equation (SWE) discretized by the finite volume method in the OpenTELEMAC computational tool (Artelia et al., 2021). TELEMAC-2D was used because the behavior of an urban flood can be represented two-dimensionally, as the horizontal extension is much greater than the vertical extension. Equations (1–3) present the SWE expressed in its nonconservative form (Li et al., 2019).

$$\frac{\partial h}{\partial t}+\frac{\partial (hu)}{\partial x}+\frac{\partial (hv)}{\partial y}=0 \tag{1}$$

$$\frac{\partial u}{\partial t}+u\frac{\partial u}{\partial x}+v\frac{\partial u}{\partial y}=-g\frac{\partial Z}{\partial x}+F_x+\frac{1}{h}\nabla(hv_e\nabla_u) \tag{2}$$

$$\frac{\partial v}{\partial t}+u\frac{\partial v}{\partial x}+v\frac{\partial v}{\partial y}=-g\frac{\partial Z}{\partial y}+F_y+\frac{1}{h}\nabla(hv_e\nabla_v) \tag{3}$$

where h is the flow depth; u, v are the depth-integrated velocity components in the x–y directions, respectively; Z is the free surface elevation; t is time; g is the acceleration due to gravity; F_x and F_y are source terms ignoring the Coriolis force and wind influence (sources and sinks); v_e is the effective diffusion for turbulent viscosity and dispersion. Details of the mathematical model can be found in Li et al. (2019).

TELEMAC-2D uses the Soil Conservation Service Curve Number (SCS-CN) method for the rain-runoff component and the Curve Number (CN) coefficient to describe the infiltration capacity. The main factors influencing the CN values were hydrological soil grouping, land use, hydrological and topographic conditions, and previous soil conditions (AMC). The formula for the SCS method is given by Equation (4) (Jiahong Liu et al., 2019).

$$S=25.4\left(\frac{1000}{CN}-10\right) \tag{4}$$

where S (dimensionless) is the potential maximum water-storage capacity of the soil. In terms of the physics-based model, the CN represents hydrological balances at the elementary level, where there is a loss or gain in mass depending on the CN associated with each element of the computational domain. TELEMAC-2D uses this component to determine the amount of fluid that runs off and infiltrates the membrane. The hyetogram in the.txt file extension was used to incorporate rainfall in TELEMAC-2D after including the information on the polygons associated with each CN (open TELEMAC-MASCARET, 2019).

3.2.1. Computational grid

An "unstructured" computational mesh was generated in BlueKenue64 V3.3 software (Ivana Kubat, 2019), which was then used in the TELEMCA 2D simulations. To determine the most appropriate element size (mesh independence test) that reproduced similar velocities and flood depths at the lowest computational cost, a mesh independence test was performed following the principles established by Li et al. (2018). The test was conducted with a simulation time of 30 min, calibration hyetogram, and river base flow. Fifty random points within the computational domain were selected (Fig. 4) to extract the temporal variations in velocity and depth. Seven refinements were used to test the independence. According to these criteria, the chosen mesh (refinement 2) had elements from 1 to 30 m for a total of 1,262,184 nodes and 2,523,221 elements (Table 1). The characteristics of the mesh, depth, and velocity of the flooding for each refinement of the mesh independence test are listed in Table 1. The angle of inclination of the elements is essential because it determines how adjacent cells relate to each other and thus influences the results.

3.2.2. Initial conditions

The initial conditions throughout the domain corresponded to the state of the terrain before the precipitation event (h(x,y,0) = 0), except for the wetlands, which were assigned the water depth before the flood event, and the El Ríito arm, where a constant flow was assigned. The depth was determined as the difference between the water elevation reached and the bottom elevation. The initial depth assigned in the wetlands was as follows: Mano de Dios 0.25 m; La Esperanza 1.00 m; Bocagrande 0.50 m; Laguna Salada 0.50 m. The initial conditions were obtained from Nardini and Miguez (2016) and Pérez-Montiel et al. (2022). The initial conditions of the river were established from a steady-state simulation with a constant flow of 58.51 m^3/s (Qin in Fig. 5) recorded during the event, as obtained in previous studies. (Pérez et al., 2018b). These conditions were considered for the calibration and validation events.

3.2.3. Boundary conditions and forcing conditions

Because the duration of the rainfall event is much shorter than the time at which the tide acts as a forcing force in the model, a constant sea level (0.5 m) was imposed as a boundary condition for the river mouth (Hout in Fig. 5), as obtained from CREACUA (2014). Rainfall was assigned as a mass source using hyetograms for the events of September 18 and November 29, 2011, assuming a homogeneous distribution throughout the urban sub-basin.

3.2.4. Assignment of hydraulic structures to the model

The subsurface drainage system, represented by massive drains, is shown in Fig. 5. The arithmetic average of the time series of the inflow and outflow rates (system saturation overflow) of 148 culverts (Fig. 5) was used to obtain the drain flow rate (0.00199 m^3/s). In this assignment, mass loss was assumed in the modeling, but there were no connections between the culverts that moved the flow from one point to another. Some structures in the study area, such as streets, canals, and protective levees, were included in the DTM simulation. Other structures, such as box culverts (Fig. 5), were included by defining the initial and final points in the calculation grid and establishing their physical characteristics (width, length, diameter, and roughness coefficient), as obtained from Pérez-Montiel et al. (2022).

3.2.5. Assignment of land uses

The predominant land uses in the study area were obtained from

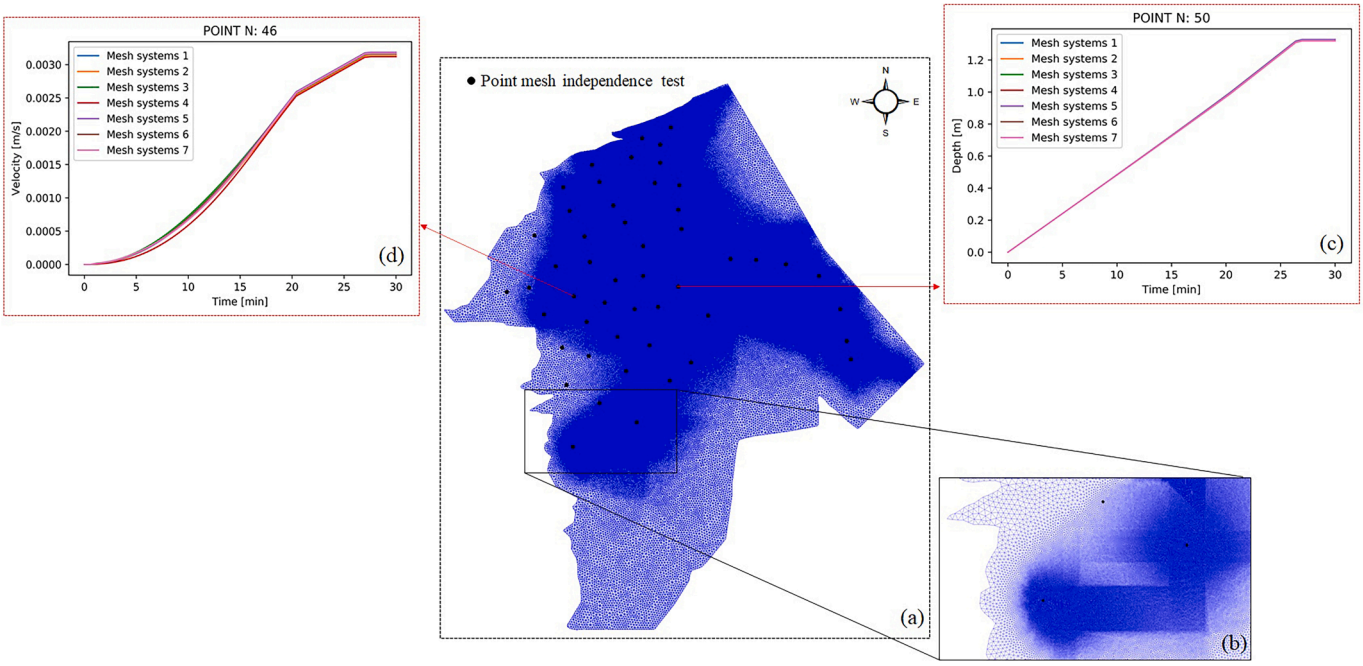


Fig. 4. Mesh independence test. (a). Computational mesh implemented in the modeling and control points for the test. (b). Characteristics of the mesh elements. (c). Evolution of flood depth at a control point. (d). Evolution of velocity at a control point.

Table 1
Mesh characteristics, velocity, and depth at each refinement of the mesh independence test.

Refinement	Mesh element sizes (m)		Number of nodes	Number of elements	Number of elements with				Velocity (m/s)	Depth (m)	Computing time
	Min.	Max.			Angle between 135° – 180°	Angle between 90° – 135°	Angle between 30° – 90°	Angle between 10° – 30°			
1	1	25	2,410,609	4,819,806	0	4,080	4,815,638	88	0.0016	1.2422	4.1 h
2	1	30	1,262,184	2,523,221	1	2,029	2,521,131	60	0.0016	1.2422	1.8 h
3	2	23	946,343	1,891,308	0	2,167	1,889,093	48	0.0015	1.2391	1.3 h
4	3	25	696,813	1,392,319	0	1,774	1,390,494	51	0.0002	1.1707	1.04 h
5	5	5	852,768	1,700,293	0	713	1,699,570	10	0.0016	1.4911	1.2 h
6	5	30	227,603	454,009	1	603	453,349	56	0.0017	1.4841	17.5 min
7	5	25	227,705	454,103	1	592	453,462	48	0.0011	1.4835	19.3 min

Nardini and Miguez (2016) and Pérez-Montiel et al. (2022) and corresponded to water (wetlands and rivers), vegetated soil, bare soil, asphalt, and buildings. These were incorporated into TELEMAC-2D using the curve number (associated with infiltration) and Manning coefficients (soil roughness). TELEMAC-2D stores these variables directly in geometric files. For the values of these parameters, we used the first approximation with information extracted from the literature (see Table 2).

3.2.6. Simulation setup

According to the hyetogram, the rainfall had a duration of 3 h for the calibration and validation events; therefore, a simulation time of 6.5 h was considered sufficient to capture the entire flooding and runoff processes in the study area. The result time interval of 150 s and the time step of 0.5 s were considered adequate for the simulations. The finite volume numerical scheme was implemented, and the "conjugate gradient" was used as the solution method.

3.3. STEP 3 - calibration strategy

SVM are supervised learning algorithms that relate well to classification and regression problems (Lee, 2021). SVM works with numerical variables; therefore, the qualitative values of the socio-hydrological variables were converted into numerical values by creating dummy variables for this study. A dummy variable is created for each possible nominal characteristic variable. The extension of the application of this tool is described in Borg & Boldt (2020) and Güven & Şimşir (2020).

Based on survey data, a hydrodynamic model, an SVM dummy, and the evaluation of performance metrics were the keys to implementing the methodology proposed in this research. To calibrate the CNs and Manning n values, traditional values based on land use and the influence of socio-hydrological variables were used. Several simulations were performed: i) reference simulation, only TELEMAC-2D with traditional information (simulation 1); ii) SVM dummy with socio-hydrological variable information (simulation 2); iii) SVM dummy with socio-hydrological variables, CN and n Manning from the literature (simulation 3); and iv) SVM dummy + TELEMAC-2D + iterative process (simulation 4). The iterative processes start from Simulation 3 to evaluate different combinations of n Manning and CN through performance metrics and select the set of values that produces the least error. These values were then assigned to TELEMAC-2D, and seven (7) simulations were performed to obtain the lowest errors.

Ranges were set for each parameter, generating 20,000 combinations for the SVM dummy. A combination of the best performance metrics was

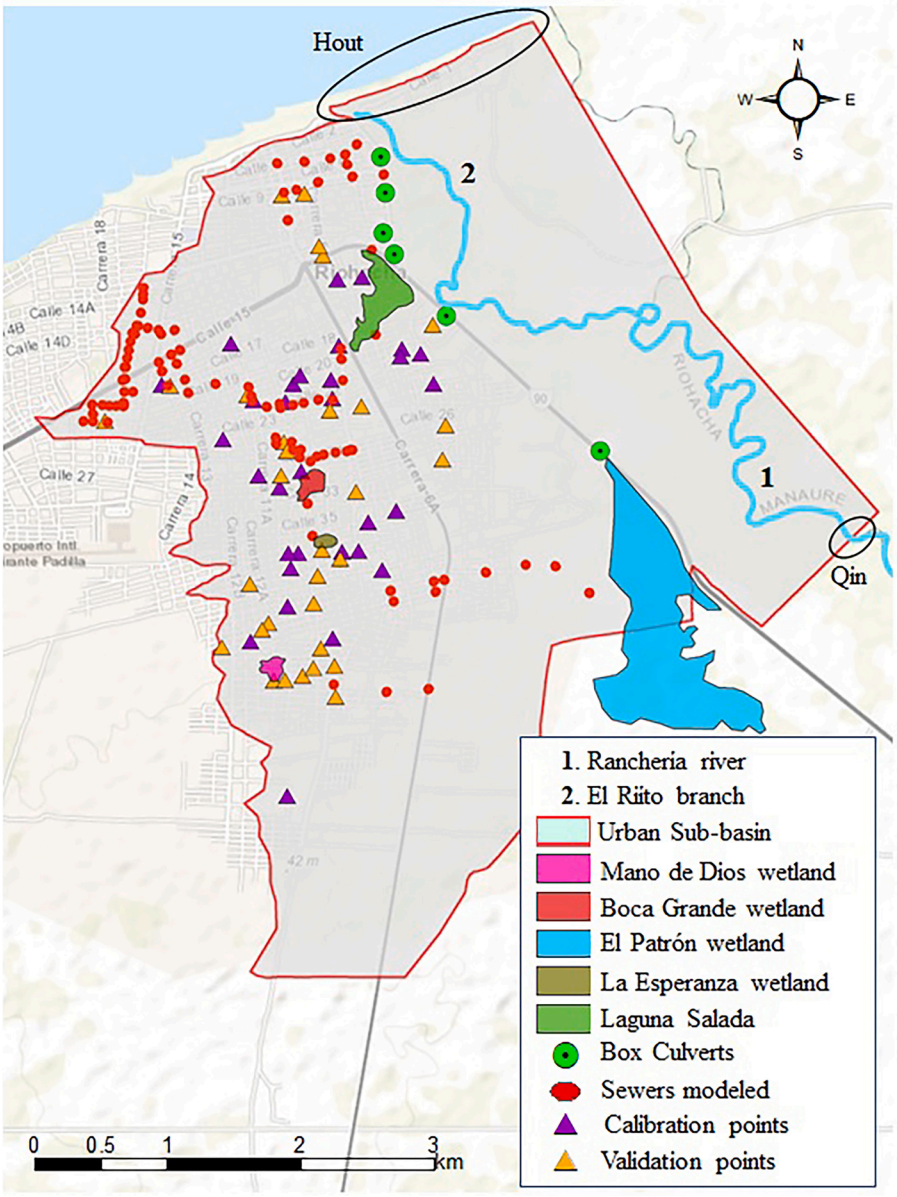


Fig. 5. Representation of wetlands, sinks, box-culverts, and points selected for calibration and validation of flood events.

Table 2
Initial values of the parameters to be evaluated in the calibration process and ranges of variation.

Surface	Land use	CN variation spectrum (%) [1]	Initial values of the CN (%) [2]	Manning's n variation spectrum [3]	Initial values of the Manning coefficient [4]
1	Water	0 - 93	100	0.025 - 0.063	0.085
2	Vegetated soil		58	0.100 - 0.160	0.500
3	Bare ground		67	0.025 - 0.065	0.300
4	Asphalt and buildings		81	0.056 - 0.094	0.085

Source: 1 (Farran et al., 2021; Im et al., 2020; Lian et al., 2020); 2 (Lian et al., 2020); 3 (Pérez-Montiel et al., 2022; Praskievicz et al., 2020); 4 (Lian et al., 2020)

used to perform the simulation using TELMAC-2D. If these metrics did not meet the fit criteria, the simulated flood depth was extracted and replaced in the SVM, and the entire iterative process was executed, limiting the ranges consistent with the results of this simulation. This process was repeated until the best fit between the measured and simulated data was obtained; these parameters were used for validation. To evaluate the best fit, we used the metrics considered by Domínguez et al. (2011), such as the mean absolute error (MAE), mean error (ME), absolute relative error (RAE), root mean square error (RMSE), and inertia root mean squared error (IRMSE).

4. Results and discussion

Using univariate (Kruskal-Wallis) and multivariate (MCA) tests applied to the survey database, 20 socio-hydrological variables other than flood depth were identified to calibrate TELEMAC-2D. The Kruskal-Wallis test identified socio-hydrological variables related to flood depth (p-value < 0.05), including the age of the house, internal slope, toilet overflow, street traffic, aqueduct service, constructed area, total area of

the property, proximity to a wetland, housing density (number of houses/m^2), distance to a pumping station, distance to the city center, paved street, and pan area. The MCA made it possible to identify socio-hydrological variables, such as the use of the dwelling, odors, runoff velocity, access to the dwelling, previous flooding, elevation of the dwelling, and slope of the soil in front of the dwelling.

Univariate and multivariate statistics have been widely used to identify the correlations between variables and flood events. Ibrahim et al. (2018) used an MCA integrated with a Geographic Information System (GIS) to identify parameters that influence flooding, such as rainfall distribution, slope, drainage density, land cover, population density, and soil. Rilo et al. (2022) used MCA to show the relationships between sets of triggers and land-use-related damage in estuarine areas, demonstrating its ability to inform flood risk management options. Rodríguez-Gaviria et al. (2019) applied the MCA technique to identify and rank the most crucial flood vulnerability variables and calculate an indicator for low-income urban territories in flood-prone areas.

Perez et al. (2018a) applied MCA to the same study area to identify the most representative housing typologies in terms of vulnerability to flood events. The application of these tools in various cases demonstrates their acceptance and popularity, which makes MCA a statistical technique for identifying socio-hydrological variables that, together with physical processes, can better represent floods and justify the values of the calibration parameters of hydrodynamic models.

4.1. Mathematical model physically-based and SVM dummy

Following model assembly, simulations were conducted for the events under study (calibration and validation). Fig. 6 shows the maps of the maximum depths present in the study area for the calibration event (September 18, 2010) with the physical conditions and socio-hydrological variables of the process. It should be noted that the northern part of the study area corresponds to the floodplain of the El Ríito branch, which acts as a buffer against the flooding of the city; therefore, high depths would be expected in this area. Depths > 3.5 m were also observed in the wetlands.

Table 3 lists the values of the CN and Manning coefficients obtained after calibration. Table 4 presents a comparison between the values obtained using the SVM and the ranges of Manning's n used in traditional investigations. These results show that the CN values of impervious areas such as water (94) and asphalt buildings (62) are within the ranges of the method, indicating that only 6% and 38% of the precipitated water infiltrates, respectively. Vegetated soil (27%) and bare ground (21%) had the highest infiltration, with values of 73% and 79%, respectively. According to Ajmal et al. (2020), Farran et al. (2021), Im et al. (2020), Lian et al. (2020), and Verma et al. (2020), the CN values obtained using the SCS method are not strictly applicable to all surfaces. In contrast to our results, Farran et al. (2021) and Lian et al. (2020) found CN values for arid soils, sparsely and heavily vegetated areas, and impervious soils within a range of 30–97% runoff.

Table 3
Initial and best-fit values using the SVM for the parameters evaluated.

Surface	Land use	Starting values of the CN (%)	Best found value for CN (%)	Starting values Manningś n	Best found value for Manning's n
1	Water	100	94	0.085	0.057
2	Vegetated soil	58	27	0.500	0.057
3	Bare ground	67	21	0.300	0.057
4	Asphalt and buildings	81	62	0.085	0.057

Table 4
Manning's n values used in urban flood studies.

Surface	Land use	Manning references			
		a	b	c	d
1	Water	0.040	0.025 - 0.063	0.029	–
2	Vegetated soil	0.100	0.100 - 0.160	0.056	0.030—0.035
3	Bare ground	0.040	0.025 - 0.065	0.040	0.030
4	Asphalt and buildings	0.016	0.056 - 0.094	0.038	0.013

Source: a (H. Li et al., 2020); b (Praskievicz et al., 2020); c (David & Schmalz, 2020); d (Demir & Keskin, 2020).

The magnitudes of the CN parameter surfaces can be explained by the influence of the entire set of socio-hydrological variables that modify or affect the normal behavior of specific land uses. For this reason, the traditional values of CN are no longer considered to be associated with traditional land use but with a surface that behaves differently owing to the influence of socio-hydrological variables (traditionally not considered), generating the behavior observed in Table 3. According to Hernández-Guzmán et al. (2021), the initial soil moisture condition is a fundamental factor that influences the behavior of the CN value. In our study, the soil was dry under the initial conditions, which also influenced the behavior of our values. This was justified by the high solar radiation and high temperatures in the study area.

Manning's coefficient is typically estimated based on judgment and experience. It also varies with changes in land cover, flow velocity, and water depth, making it challenging to determine this value (Shih & Chen, 2021). Table 4 shows that a constant value of 0.057 was obtained for different degrees of roughness in the case under study. This implies

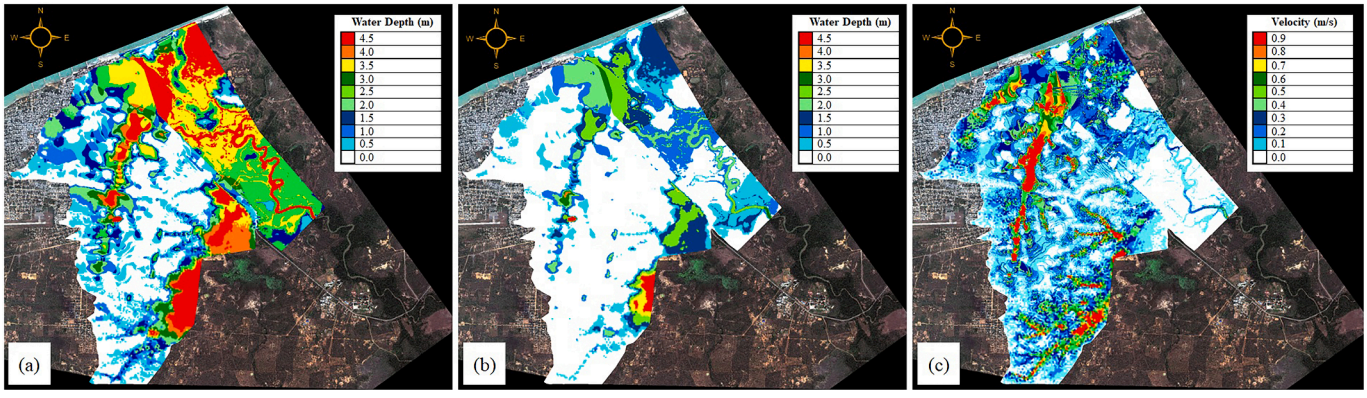


Fig. 6. Results of the modeling of the calibration event with TELEMAC-2D. (a). TELEMAC-2D with traditional information; (b). Maximum flood depths with SVM dummy + TELEMAC-2D + iterative process; (c). Maximum velocities with SVM dummy + TELEMAC-2D + iterative process.

that the model is not as susceptible to Manning's n as it is to CN owing to the low velocities presented in the flood event. Because Manning is a parameter that varies with velocity and depth, this behavior is explained by the following: i) because Riohacha has a flat topography, it is corroborated that velocity has little influence on flooding, causing the storage of large volumes of mass that generate effects due to the depth they reach in some sectors; ii) the influence of socio-hydrological variables, such as paved streets and housing density, means that the fluid does not present as much resistance; and iii) the presence of large areas without vegetation. These factors caused the forces to balance, and an average value of n was obtained throughout the simulation area.

However, Fig. 6(b) shows that the alluvial plain of the Riíto arm functions as a water storage area, which helps to dissipate runoff and lower city levels. However, this process occurs slowly because the culverts connecting the city to the floodplain are too small to transfer water quickly. However, this flow from the urban area to the alluvial plain and the overflow of the El Riíto branch transfers and increases the problem of Villa Fatima urbanization (see Fig. 1), where flood depths in low areas exceed one meter. Table 5 lists the flood depths obtained during the final calibration of the physics-based model. Fig. 7 shows the values of the metrics evaluated in each simulation.

Fig. 7 shows that for Simulation 1, the evaluated metrics presented higher errors than in the other simulated cases. The RMSE reflects that in both calibration (0.48 m) and validation (0.63 m), the model is as good as the mean of the data, which means that the observations cannot be correctly predicted. Consequently, this behavior is observed in IRMSE, with calibration values of 1.33 and validation of 2.19, reflecting that the process trend produces more information than the model, a sign of poor fit. The same behavior was observed for the MAE and RMSE.

For Simulation 2, the differences between the observed and simulated data continued to be marked, specifically for validation. The IRMSE for the calibration (0.57) and validation (0.98) showed errors greater than 50 cm. These results indicate that the model could only produce, on average, 20% more information than the process trend, making it unacceptable. In contrast, Fig. 7 shows that for Simulations 2 and 3, the metrics exhibit the same behavior, indicating that including the simulated flood depth as a new variable in the SVM does not provide relevant information. Simulation 3 required a GIS algorithm to specialize, interpolate, and spatially visualize flooding behavior. Similarly, this tool does not allow the prediction of future events. Another weakness of this process is that if it is required to spatialize the flood along the entire computational domain, many observations with similar information are required, which is not commonly available.

From the articulation between SVM and TELEMAC-2D (simulation 4), Fig. 7 shows the results obtained for MAE and ME in calibration (0.27 and 0.17 m) and validation (0.13 and 0.04 m). Unlike simulation 1, this shows a substantial improvement, especially for validation. Similar behavior was observed for RMSE and IRMSE, with values of 0.33 m and 0.92 m for calibration and 0.18 m and 0.55 m for validation, respectively. The best performance of the model was presented in Simulation 4, specifically in the validation, which, despite not having the same behavior for the calibration, managed to produce 45% more information than the data trend. In terms of socio-hydrological variables, Simulation 4 was the best fit (as shown in Fig. 6(b)).

The most commonly used metric to evaluate the fit of a model is the RMSE, which is closer to zero, and the error between the observed and simulated data is minimal. In contrast, Ghimire et al. (2022), (Mali & Kuiry 2020), and Shih and Chen (2021) obtained values ranging from 0.096 m to 1.2 m, indicating that the proposed methodology generates scientifically valid results. Pérez-Montiel et al. (2022), in a case study of the city of Riohacha with traditional physics-based models and methodologies, reported RMSE values ranging from 0.062 m to 0.40 m, which ratifies that the proposed methodology manages to represent flood events acceptably. A point of inflection between both studies is that in the one reported by Pérez-Montiel et al. (2022), approximately 50 simulations were performed for the calibration of the hydrodynamic model, whereas in our case, it was achieved with 7 iterative processes, which significantly reduces the operational and computational costs.

Table 5
Flood depth results obtained with the methodological proposal developed in the research.

# of selected survey	Surveyed flood depth (m)	Simulated flood depth (m)	Error	MAE	ME	RSME	IRMSE
1	0.50	0.17	0.33				
2	1	0.22	0.78				
3	1.06	1.45	−0.39				
4	0.44	0.75	−0.31				
5	0.76	0.10	0.66				
6	0.29	0.28	0.01				
7	0.60	0.14	0.46				
8	0.40	0.26	0.14				
9	0.76	0.38	0.38				
10	0.20	0.05	0.15				
11	0.32	0.20	0.12				
12	0.58	0.21	0.37				
13	0.13	0.19	−0.06				
14	0.19	0.14	0.05				
15	0.36	0.16	0.20				
16	0.21	0.38	−0.17	0.27	0.17	0.33	0.34
17	0.21	0.08	0.13				
18	0.46	0.78	−0.32				
19	0.63	0.34	0.29				
20	0.52	0.16	0.36				
21	0.55	0.32	0.23				
22	0.11	0.35	−0.24				
23	0.52	0.12	0.40				
24	0.17	0.17	0.00				
25	0.20	0.12	0.08				
26	0.01	0.18	−0.17				
27	0.68	0.03	0.65				
28	0.94	0.56	0.38				
29	0.20	0.14	0.06				
30	0.73	0.16	0.57				
31	0.27	0.12	0.15				
32	0.26	0.09	0.17				

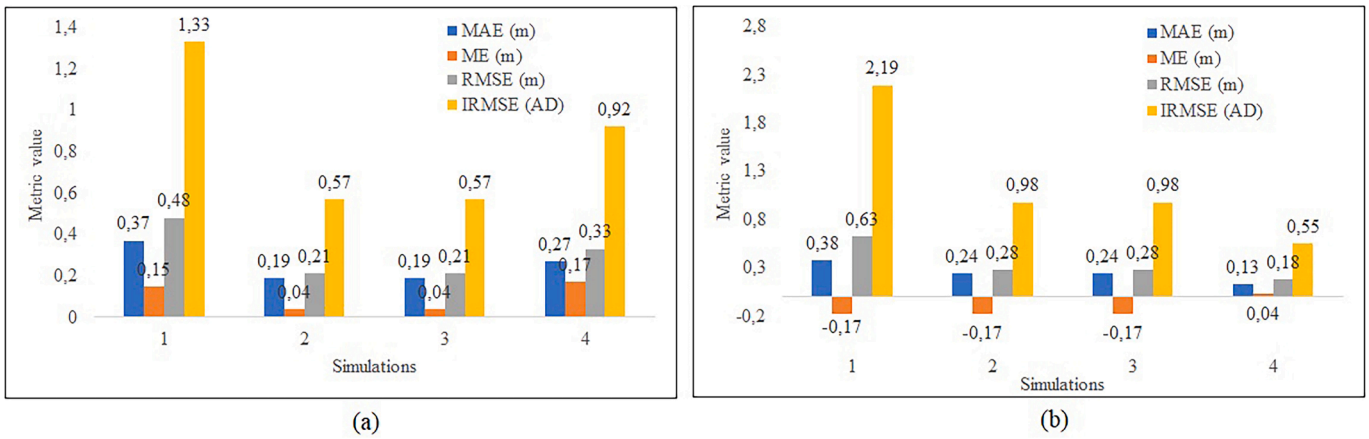


Fig. 7. Results of the different metrics implemented to evaluate the adjustment of the models in: (a). Calibration process; (b). Validation process.

The methodology proposed in this research, which includes socio-hydrological variables, is presented as a strategy for calibrating physics-based models. Traditional calibration requires a trial-and-error method to determine the optimal parameter values, which must be varied directly at the modeler's discretion. The hydrodynamic model has a high computational cost, especially in large domains, which conditions the time depending on the capabilities of the available hardware. In contrast, SVMs that consider socio-hydrological variables can be trained in minutes, which allows the modeler to have a more reasonable view of the ranges in which the optimal values of the parameters can be found, considerably reducing the number of simulations. A fundamental aspect of the research was the uncertainty of the survey information because it was applied 4 years after the occurrence of the flood events studied. The uncertainty was not evaluated in detail but was considered in the selection criteria of the survey database (Fig. 3).

5. Conclusion

The objective of this study was to propose a methodological approach for urban flood modeling that integrates numerical tools based on physical and socio-hydrological variables. TELEMAC-2D is a flood simulation tool that adequately represents the physical process of a flood event and provides valuable information for risk management decision-makers. However, it is recommended to use alternative models, such as DELFT2D-FLOW, IBER, iRIC, and HEC-RAS-2D, which can be integrated with statistically based models when considering socio-hydrological variables.

The SVM dummy is a useful and practical tool for integrating physics-based and statistical models, providing unlimited combinations of parameters used for calibration and simplifying the inclusion of quantitative and qualitative variables, thus reducing operational costs and computational time. In future research, other autonomous learning tools (e.g., Bayesian networks, random forests, decision trees, and neural networks) could be used.

Urban flooding can be better represented by integrating socio-hydrological variables into physics-based models. Therefore, for future research, it is recommended to i) replicate the proposed methodology in other areas with scarce information, ii) implement another type of traditional optimization algorithm within the SVM, iii) use a DTM with higher resolution that can better represent the reality of the urban fabric, such as streets, sidewalks, and unevenness of houses, among others, and iv) apply the methodological proposal in other case studies.

The methodology is proposed as a one-time calibration strategy for physics-based models. The joint application of TELEMAC-2D and SVM is performed at the time of using the calibration process, then, the hydrodynamic model is implemented to evaluate any scenario. It is essential that this process is carried out by a qualified person with knowledge in both tools.

CRediT authorship contribution statement

Leyner Cardenas-Mercado: Conceptualization, Methodology, Investigation, Data curation, Resources, Writing – original draft, Visualization. **Jorge Escobar-Vargas:** Conceptualization, Methodology, Writing – original draft. **Jhonny I. Pérez-Montiel:** Conceptualization, Methodology, Resources, Writing – original draft, Visualization. **Andres Torres:** Conceptualization, Methodology, Data curation, Writing – original draft, Visualization.

Declaration of Competing Interest

The authors declare that they have no known competing financial interests or personal relationships that could have appeared to influence the work reported in this paper.

Data availability

The data that has been used is confidential.

Acknowledgments

This research was carried out thanks to the support of the Pontificia Universidad Javeriana; CREACUA Foundation (Riohacha-Colombia), which provided the necessary information from the original MODCEL project "Adaptación Urbana Verde Frente a Inundaciones con el Soporte de la Modelación Matemática y del Software MODCEL en Riohacha, La Guajira, Colombia"; Universidad de La Guajira-Colombia; Minciencias (Ministry of Science, Technology and Innovation); and Colfuturo (Foundation for the Future of Colombia) for all the support provided in the completion of the master's studies of the National Master's call - 810. We acknowledge the support of Ph.D. Jairo Escobar, who adapted the required information and followed it up during the work execution.

References

Abebe, Y.A., Ghorbani, A., Nikolic, I., Vojinovic, Z., Sanchez, A., 2019. A coupled flood-agent-institution modelling (CLAIM) framework for urban flood risk management. Environ. Model. Softw. 111 (October), 483–492. https://doi.org/10.1016/j.envsoft.2018.10.015.

Agonafir, C., Lakhankar, T., Khanbilvardi, R., Krakauer, N., Radell, D., Devineni, N., 2022. A machine learning approach to evaluate the spatial variability of New York City's 311 street flooding complaints. Comput. Environ. Urban Syst. 97 (February), 101854 https://doi.org/10.1016/j.compenvurbsys.2022.101854.

Ajmal, M., Waseem, M., Kim, D., Kim, T.-W., 2020. A pragmatic slope-adjusted curve number model to reduce uncertainty in predicting flood runoff from steep watersheds. Water 12 (5), 1469. https://doi.org/10.3390/w12051469.

Anh, P.T., Ngoc, N.T.B., 2019. Public participatory role in urban flood risk management of Ho Chi Minh City - Vietnam: from awareness to action. South Asian J. Soc. Studies Econ. 4 (4), 1–10. https://doi.org/10.9734/sajsse/2019/v4i430133.

Anupam, S., Pani, P., 2020. Flood forecasting using a hybrid extreme learning machine-particle swarm optimization algorithm (ELM-PSO) model. Model. Earth Syst. Environ. 6 (1), 341–347. https://doi.org/10.1007/s40808-019-00682-z.

Artelia, F. S. F., BAW, F. W. E. and R. I., CEREMA, Centre for Studies and Expertise on Risks, the Environment, M. and U. P., CERFACS, C. E. de R. et de F. A. en C. S., UHRI, S. and T. F. C., EDF, É. de F., & HR Wallingford, H. R. S. (2021, July 4). *TELEMAC-MASCARET*. http://www.opentelemac.org/index.php/22-introduction/83-welcome-to-telemac.

Aung, N.N., Htwe, S.S., Sein, K.K., Aung, L.L., 2019. The impact of floods on the socio-economic activities of Yangon. In: Population, Development, and the Environment. Springer Singapore, pp. 255–271. https://doi.org/10.1007/978-981-13-2101-6_15.

Blair, P., Buytaert, W., 2016. Socio-hydrological modelling: a review asking "why, what and how?&quot. Hydrol. Earth Syst. Sci. 20 (1), 443–478. https://doi.org/10.5194/hess-20-443-2016.

Borg, A., Boldt, M., 2020. Using VADER sentiment and SVM for predicting customer response sentiment. Expert Syst. Appl. 162, 113746 https://doi.org/10.1016/j.eswa.2020.113746.

Buarque, A.C.S., Souza, C.F., Souza, F.A.A., Mendiondo, E.M., 2021. Urban flood risk under global changes: a socio-hydrological and cellular automata approach in a Brazilian catchment. Hydrol. Sci. J. 66 (14), 2011–2021. https://doi.org/10.1080/02626667.2021.1977813.

Campuzano, O.C.P., Roldán, G., Torres Abello, A.E., Lara-Borrero, J., Galarza-Molina, S. L., Giraldo Osorio, J.D., Duarte, M., Fajardo Ruiz, S.M., Montoya Jaramillo, L.J., Daniel, C., 2015. Desafíos del agua urbana en las américas - Perspectivas de las Academias de Ciencias. Desafíos del agua urbana en las américas - Perspectivas de las Academias de Ciencias. https://unesdoc.unesco.org/ark:/48223/pf0000245202.

CDGRD, 2019. *Plan Distrital de Gestión del Riesgo de Desastres – Distrito de Riohacha – La Guajira*. http://repositorio.gestiondelriesgo.gov.co/handle/20.500.11762/28331.

Ciullo, A., Viglione, A., Castellarin, A., Crisci, M., Di Baldassarre, G., 2017. Socio-hydrological modelling of flood-risk dynamics: comparing the resilience of green and technological systems. Hydrol. Sci. J. 62 (6), 880–891. https://doi.org/10.1080/02626667.2016.1273527.

CREACUA. (2013). Proyecto: “Adaptación Urbana Verde frente a inundaciones con el soporte de la modelación matemática y del software MODCEL en Riohacha, La Guajira, Colombia”; Convenio de cooperación N° 9677-04-1047-2013; CREACUA: Riohacha, Colombia. http://modcelrhcdatos.wixsite.com/modcel-riohacha/avance.

CREACUA. (2014). Proyecto: “Adaptación Urbana Verde frente a inundaciones con el soporte de la modelación matemática y del software MODCEL en Riohacha, La Guajira, Colombia”; Convenio de cooperación N° 9677-04-1047-2013; CREACUA: Riohacha, Colombia. Componente hidrología. https://creacua.wixsite.com/creacua/projects.

Dahri, N., Abida, H., 2020. Causes and impacts of flash floods: case of Gabes City, Southern Tunisia. Arab. J. Geosci. 13 (4), 176. https://doi.org/10.1007/s12517-020-5149-7.

David, A., Schmalz, B., 2020. Flood hazard analysis in small catchments: Comparison of hydrological and hydrodynamic approaches by the use of direct rainfall. J. Flood Risk Manage. 13 (4) https://doi.org/10.1111/jfr3.12639.

De Goede, E.D., 2020. Historical overview of 2D and 3D hydrodynamic modelling of shallow water flows in the Netherlands. Ocean Dyn. 70 (4), 521–539. https://doi.org/10.1007/s10236-019-01336-5.

Demir, V., Keskin, A.Ü., 2020. Obtaining the Manning roughness with terrestrialremote sensing technique and flood modeling using FLO-2D. Geofizika 37 (2), 131–156. https://doi.org/10.15233/gfz.2020.37.9.

Di Baldassarre, G., Viglione, A., Carr, G., Kuil, L., Yan, K., Brandimarte, L., Blöschl, G., 2015. Debates-Perspectives on socio-hydrology: Capturing feedbacks between physical and social processes. Water Resour. Res. 51 (6), 4770–4781. https://doi.org/10.1002/2014WR016416.

Domínguez, E., Dawson, C.W., Ramírez, A., Abrahart, R.J., 2011. The search for orthogonal hydrological modelling metrics: a case study of 20 monitoring stations in Colombia. J. Hydroinf. 13 (3), 429–442. https://doi.org/10.2166/hydro.2010.116.

Du, E., Wu, F., Jiang, H., Guo, N., Tian, Y., Zheng, C., 2023. Development of an integrated socio-hydrological modeling framework for assessing the impacts of shelter location arrangement and human behaviors on flood evacuation processes. Hydrol. Earth Syst. Sci. 27 (7), 1607–1626. https://doi.org/10.5194/hess-27-1607-2023.

Esmaelian, M., Tavana, M., Di Caprio, D., Ansari, R., 2017. A multiple correspondence analysis model for evaluating technology foresight methods. Technol. Forecast. Soc. Chang. 125, 188–205. https://doi.org/10.1016/j.techfore.2017.07.022.

Farran, M.M., Elfeki, A., Elhag, M., Chaabani, A., 2021. A comparative study of the estimation methods for NRCS curve number of natural arid basins and the impact on flash flood predications. Arab. J. Geosci. 14 (2), 121. https://doi.org/10.1007/s12517-020-06341-3.

Genova, P., Wei, Y., 2023. A socio-hydrological model for assessing water resource allocation and water environmental regulations in the Maipo River basin. J. Hydrol. 617, 129159 https://doi.org/10.1016/j.jhydrol.2023.129159.

Ghimire, E., Sharma, S., Lamichhane, N., 2022. Evaluation of one-dimensional and two-dimensional HEC-RAS models to predict flood travel time and inundation area for flood warning system. ISH J. Hydraul. Eng. 28 (1), 110–126. https://doi.org/10.1080/09715010.2020.1824621.

Güven, İ., Şimşir, F., 2020. Demand forecasting with color parameter in retail apparel industry using artificial neural networks (ANN) and support vector machines (SVM) methods. Comput. Ind. Eng. 147 (July), 106678 https://doi.org/10.1016/j.cie.2020.106678.

Habibi, H., Seo, D.-J., 2018. Simple and modular integrated modeling of storm drain network with gridded distributed hydrologic model via grid-rendering of storm drains for large urban areas. J. Hydrol. 567 (October), 637–653. https://doi.org/10.1016/j.jhydrol.2018.10.037.

Hernández-Guzmán, R., Ruiz-Luna, A., Mendoza, E., 2021. Sara4r: an R graphical user interface (GUI) to estimate watershed surface runoff applying the NRCS – curve number method. J. Hydroinf. 23 (1), 76–87. https://doi.org/10.2166/hydro.2020.087.

Ibrahim, B.A., Tiki, D., Mamdem, L., Leumbe, O.L., Bitom, D., Lazar, G., 2018. MultiCriteria analysis (MCA) approach and GIS for flood risk assessment and mapping in Mayo Kani Division, Far North Region of Cameroon. Internat. J. Adv. Remote Sens. GIS 7 (1), 2793–2808. https://doi.org/10.23953/cloud.ijarsg.375.

Im, S., Lee, J., Kuraji, K., Lai, Y.-J., Tuankrua, V., Tanaka, N., Gomyo, M., Inoue, H., Tseng, C.-W., 2020. Soil conservation service curve number determination for forest cover using rainfall and runoff data in experimental forests. J. For. Res. 25 (4), 204–213. https://doi.org/10.1080/13416979.2020.1785072.

Juez, C., Murillo, J., García-Navarro, P., 2014. A 2D weakly-coupled and efficient numerical model for transient shallow flow and movable bed. Adv. Water Resour. 71, 93–109. https://doi.org/10.1016/j.advwatres.2014.05.014.

Khalifa, M., Elagib, N.A., Ahmed, B.M., Ribbe, L., Schneider, K., 2020. Exploring socio-hydrological determinants of crop yield in under-performing irrigation schemes: pathways for sustainable intensification. Hydrol. Sci. J. 65 (2), 153–168. https://doi.org/10.1080/02626667.2019.1688333.

Kim, B., Sanders, B.F., Schubert, J.E., Famiglietti, J.S., 2014. Mesh type tradeoffs in 2D hydrodynamic modeling of flooding with a Godunov-based flow solver. Adv. Water Resour. 68, 42–61. https://doi.org/10.1016/j.advwatres.2014.02.013.

Ivana Kubat. (2019, March 19). *Blue Kenue™: software tool for hydraulic modellers*. https://nrc.canada.ca/en/research-development/products-services/software-applications/blue-kenuetm-software-tool-hydraulic-modellers.

Kundu, P.K., Cohen, I.M., Dowling, D.R., 2015. Fluid Mechanics. Elsevier Science. https://books.google.com.co/books?id=EehDBAAAQBAJ.

Lee, S., 2021. Monte Carlo simulation using support vector machine and kernel density for failure probability estimation. Reliab. Eng. Syst. Saf. 209 (January), 107481 https://doi.org/10.1016/j.ress.2021.107481.

Li, H., Gao, H., Zhou, Y., Xu, C.-Y., Ortega, M.R.Z., Sælthun, N.R., 2020. Usage of SIMWE model to model urban overland flood: a case study in Oslo. Hydrol. Res. 51 (2), 366–380. https://doi.org/10.2166/nh.2020.068.

Li, L., Mei, S., Wang, Yan, 2019. Comparative analysis of building representations in TELEMAC-2D for flood inundation in idealized urban districts. Water 11 (9), 1840. https://doi.org/10.3390/w11091840.

Li, Z., Miao, Z., Shen, X., Li, J., 2018. Prevention of boiler performance degradation under large primary air ratio scenario in a 660 MW brown coal boiler. Energy 155, 474–483. https://doi.org/10.1016/j.energy.2018.05.008.

Lian, H., Yen, H., Huang, J.-C., Feng, Q., Qin, L., Bashir, M.A., Wu, S., Zhu, A.-X., Luo, J., Di, H., Lei, Q., Liu, H., 2020. CN-China: Revised runoff curve number by using rainfall-runoff events data in China. Water Res. 177, 115767 https://doi.org/10.1016/j.watres.2020.115767.

Liu, J., Li, Z., Mei, C., Wang, K., Zhou, G., 2019. Urban flood analysis for different design storm hyetographs in Xiamen Island based on TELEMAC-2D. Chin. Sci. Bull. 64 (19), 2055–2066. https://doi.org/10.1360/N972018-01180.

Liu, J., Xiong, J., Cheng, W., Li, Y., Cao, Y., He, Y., Duan, Y., He, W., Yang, G., 2021. Assessment of flood susceptibility using support vector machine in the belt and road region. Nat. Hazards Earth Syst. Sci. Discuss. 2021, 1–37. https://doi.org/10.5194/nhess-2021-80.

Liu, J., Wang, J., Xiong, J., Cheng, W., Li, Y., Cao, Y., He, Y., Duan, Y., He, W., Yang, G., 2022. Assessment of flood susceptibility mapping using support vector machine, logistic regression and their ensemble techniques in the Belt and Road region. Geocarto Int. 37 (25), 9817–9846. https://doi.org/10.1080/10106049.2022.2025918.

Lu, Q., Wai, O.W.H., 1998. An efficient operator splitting scheme for three-dimensional hydrodynamic computations. Internat. J. Num. Methods Fluids 26 (7), 771–789. https://doi.org/10.1002/(SICI)1097-0363(19980415)26:7<771::AID-FLD672>3.0.CO;2-7.

Luo, P., Luo, M., Li, F., Qi, X., Huo, A., Wang, Z., He, B., Takara, K., Nover, D., Wang, Y., 2022. Urban flood numerical simulation: Research, methods and future perspectives. Environ. Model. Softw. 156, 105478 https://doi.org/10.1016/j.envsoft.2022.105478.

Mali, V.K., Kuiry, S.N., 2020. Experimental and numerical study of flood in a river-network-floodplain set-up. J. Hydraul. Res. 58 (6), 938–956. https://doi.org/10.1080/00221686.2019.1698471.

Martins, R., Leandro, J., Djordjević, S., 2018. Influence of sewer network models on urban flood damage assessment based on coupled 1D/2D models. J. Flood Risk Manage. 11, S717–S728. https://doi.org/10.1111/jfr3.12244.

Massuel, S., Riaux, J., Molle, F., Kuper, M., Ogilvie, A., Collard, A.-L., Leduc, C., Barreteau, O., 2018. Inspiring a broader socio-hydrological negotiation approach with interdisciplinary field-based experience. Water Resour. Res. 54 (4), 2510–2522. https://doi.org/10.1002/2017WR021691.

Mignot, E., Li, X., Dewals, B., 2019. Experimental modelling of urban flooding: A review. J. Hydrol. 568 (November), 334–342. https://doi.org/10.1016/j.jhydrol.2018.11.001.

Minano, A., Thistlethwaite, J., Henstra, D., Scott, D., 2021. Governance of flood risk data: A comparative analysis of government and insurance geospatial data for identifying properties at risk of flood. Comput. Environ. Urban Syst. 88 (March), 101636 https://doi.org/10.1016/j.compenvurbsys.2021.101636.

Monge, J. F. (2019). *The Concordance coefficient: An alternative to the Kruskal-Wallis test*. 1–34. http://arxiv.org/abs/1912.12880.

Mostert, E., 2018. An alternative approach for socio-hydrology: case study research. Hydrol. Earth Syst. Sci. 22 (1), 317–329. https://doi.org/10.5194/hess-22-317-2018.

Nardini, A., Miguez, G.M., 2016. An Integrated Plan to Sustainably Enable the City of Riohacha (Colombia) to Cope with Increasing Urban Flooding, while Improving Its Environmental Setting. Sustainability 8 (3), 198. https://doi.org/10.3390/su8030198.

Neal, J., Villanueva, I., Wright, N., Willis, T., Fewtrell, T., Bates, P., 2012. How much physical complexity is needed to model flood inundation? Hydrol. Process. 26 (15), 2264–2282. https://doi.org/10.1002/hyp.8339.

Ning, L., Yamazaki, Y., Roeber, V., Cheung, K.F., Chock, G., 2018. Probabilistic mapping of storm-induced coastal inundation for climate change adaptation. Coast. Eng. 133, 126–141. https://doi.org/10.1016/j.coastaleng.2017.12.013.

Nkwunonwo, U.C., Whitworth, M., Baily, B., 2019. Urban flood modelling combining cellular automata framework with semi-implicit finite difference numerical formulation. J. Afr. Earth Sc. 150 (September 2018), 272–281. https://doi.org/10.1016/j.jafrearsci.2018.10.016.

open TELEMAC-MASCARET. (2019). *TELEMAC-2D user manual.* TELEMAC-2D. http://www.opentelemac.org/index.php/manuals/viewcategory/13-telemac-2d.

Pathak, M.A., 2014. Exploratory Data Analysis. In: *Beginning Data Science with R*. Springer International Publishing, pp. 61–85. https://doi.org/10.1007/978-3-319-12066-9_5.

Pérez, J., Escobar, J., Fragozo, J., 2018b. Modelación Hidráulica 2D de Inundaciones en Regiones con Escasez de Datos. El Caso del Delta del Río Ranchería, Riohacha-Colombia. Información Tecnológica 29 (4), 143–156. https://doi.org/10.4067/S0718-07642018000400143.

Perez, J.I., Nardini, A., Zuñiga, Y.P., 2018a. Identificación Multiatributo de Tipologías de Viviendas Vulnerables a Inundaciones en Riohacha, La Guajira-Colombia. Información Tecnológica 29 (5), 187–202. https://doi.org/10.4067/S0718-07642018000500187.

Pérez-Montiel, J.I., Cardenas-Mercado, L., Nardini, A.G.C., 2022. Flood modeling in a coastal town in Northern Colombia: comparing MODCEL vs. IBER. Water 14 (23), 3866. https://doi.org/10.3390/w14233866.

Praskievicz, S., Carter, S., Dhondia, J., Follum, M., 2020. Flood-inundation modeling in an operational context: sensitivity to topographic resolution and Manning's n. J. Hydroinf. 22 (5), 1338–1350. https://doi.org/10.2166/hydro.2020.005.

Rilo, A., Tavares, A.O., Freire, P., Zêzere, J.L., Haigh, I.D., 2022. Improving estuarine flood risk knowledge through documentary data using multiple correspondence analysis. Water 14 (19), 3161. https://doi.org/10.3390/w14193161.

Rodríguez-Gaviria, E.M., Ochoa-Osorio, S., Builes-Jaramillo, A., Botero-Fernández, V., 2019. Computational bottom-up vulnerability indicator for low-income flood-prone urban areas. Sustainability 11 (16), 4341. https://doi.org/10.3390/su11164341.

Russo, B., Sunyer, D., Velasco, M., Djordjević, S., 2015. Analysis of extreme flooding events through a calibrated 1D/2D coupled model: the case of Barcelona (Spain). J. Hydroinf. 17 (3), 473–491. https://doi.org/10.2166/hydro.2014.063.

Shen, Y., Morsy, M.M., Huxley, C., Tahvildari, N., Goodall, J.L., 2019. Flood risk assessment and increased resilience for coastal urban watersheds under the combined impact of storm tide and heavy rainfall. J. Hydrol. 579 (June), 124159 https://doi.org/10.1016/j.jhydrol.2019.124159.

Shih, S., Chen, P., 2021. Identifying tree characteristics to determine the blocking effects of water conveyance for natural flood management in urban rivers. J. Flood Risk Manage. 14 (4) https://doi.org/10.1111/jfr3.12742.

Song, S., Wang, S., Fu, B., Dong, Y., Liu, Y., Chen, H., Wang, Y., 2021. Improving representation of collective memory in socio-hydrological models and new insights into flood risk management. J. Flood Risk Manage. 14 (1) https://doi.org/10.1111/jfr3.12679.

Tehrany, M.S., Pradhan, B., Jebur, M.N., 2014. Flood susceptibility mapping using a novel ensemble weights-of-evidence and support vector machine models in GIS. J. Hydrol. 512, 332–343. https://doi.org/10.1016/j.jhydrol.2014.03.008.

Tehrany, M.S., Pradhan, B., Jebur, M.N., 2015. Flood susceptibility analysis and its verification using a novel ensemble support vector machine and frequency ratio method. Stoch. Env. Res. Risk A. 29 (4), 1149–1165. https://doi.org/10.1007/s00477-015-1021-9.

Verma, S., Singh, P.K., Mishra, S.K., Singh, V.P., Singh, V., Singh, A., 2020. Activation soil moisture accounting (ASMA) for runoff estimation using soil conservation service curve number (SCS-CN) method. J. Hydrol. 589, 125114 https://doi.org/10.1016/j.jhydrol.2020.125114.

Wan Mohtar, W.H.M., Abdullah, J., Abdul Maulud, K.N., Muhammad, N.S., 2020. Urban flash flood index based on historical rainfall events. Sustain. Cities Soc. 56 (November 2019), 102088 https://doi.org/10.1016/j.scs.2020.102088.

Yan, J., Jin, J., Chen, F., Yu, G., Yin, H., Wang, W., 2018. Urban flash flood forecast using support vector machine and numerical simulation. J. Hydroinf. 20 (1), 221–231. https://doi.org/10.2166/hydro.2017.175.

Zambrano, L., Pacheco-Muñoz, R., Fernández, T., 2018. Influence of solid waste and topography on urban floods: The case of Mexico City. Ambio 47 (7), 771–780. https://doi.org/10.1007/s13280-018-1023-1.

Zhang, S.-Z., Yang, N.-H., Wang, X.-K., 2002. Construction and application of Bayesian networks in flood decision supporting system. Proc. Internat. Conf. Machine Learn. Cybernet. 2 (November), 718–722. https://doi.org/10.1109/ICMLC.2002.1174468.